Supporting Information

Silicon-Core Carbon-Shell Nanoparticles for Lithium-ion Batteries: Rational Comparison Between Amorphous and Graphitic Carbon Coatings

*Giorgio Nava[1], Joseph Schwan[1], Matthew G. Boebinger[3], Matthew T. McDowell[3,4], Lorenzo Mangolini[1,2] **

[1]Department of Mechanical Engineering, University of California, Riverside, 900 University Ave, Riverside, California 92521.

[2]Department of Materials Science, University of California, Riverside, 900 University Ave, Riverside, California 92521.

[3]School of Materials Science and Engineering, Georgia Institute of Technology, 771 Ferst Drive, Atlanta, GA, 30332.

[4]George W. Woodruff School of Mechanical Engineering, Georgia Institute of Technology, 801 Ferst Drive, Atlanta, GA 30332.

* email: lmangolini@engr.ucr.edu

Keywords: Silicon, Amorphous Carbon, Graphitic Carbon, Chemical Vapor Deposition, Lithium-ion batteries, Additive.

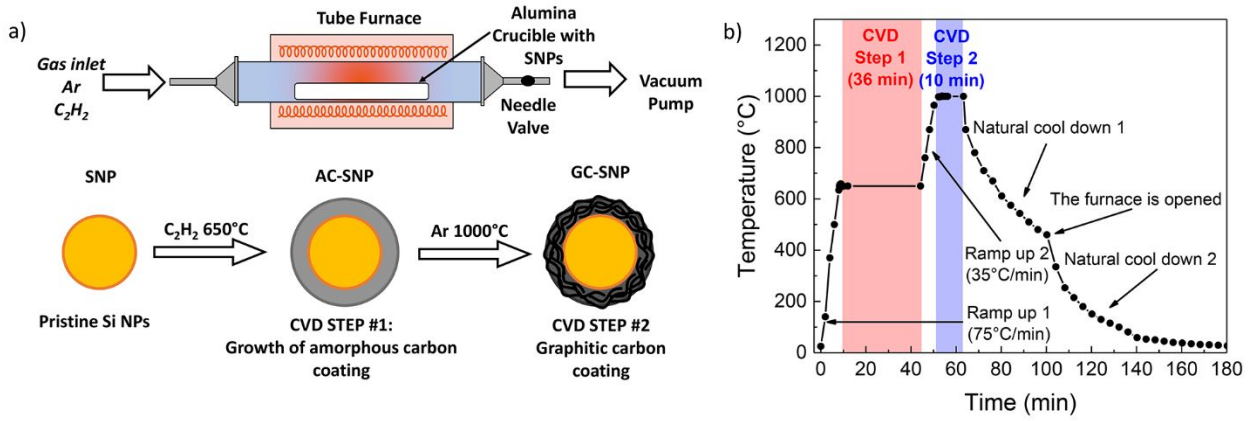

Figure s1. Schematic of the CVD setup used for the synthesis of the silicon-carbon composites and depiction of the effect of the two CVD steps on the carbon coating wrapping the Si particles (a). In the first low temperature step, C_2H_2 is dissociated at moderate temperature (650°C), producing silicon particles wrapped with a conformal coating of amorphous carbon. This first composite is labelled as AC-SNP. In the second step the composite is annealed in Ar at high temperature (1000°C), inducing the complete graphitization of the carbon coating. This second type of composite is labeled GC-SNP. Temperature profile of the CVD process (b).

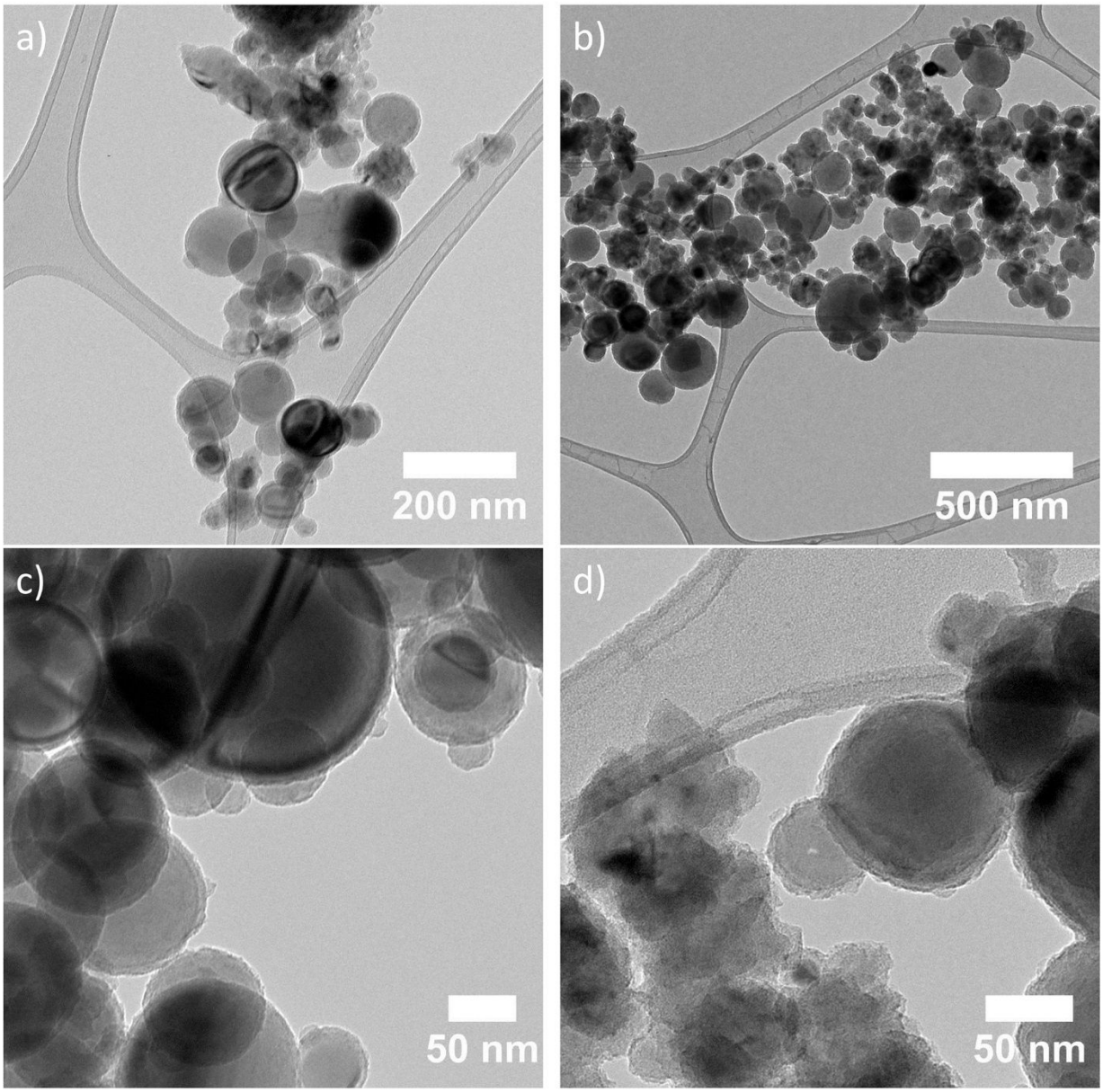

Figure s2. Low magnification TEM micrographs of AC-SNP (a, c) and GC-SNP (b, d).

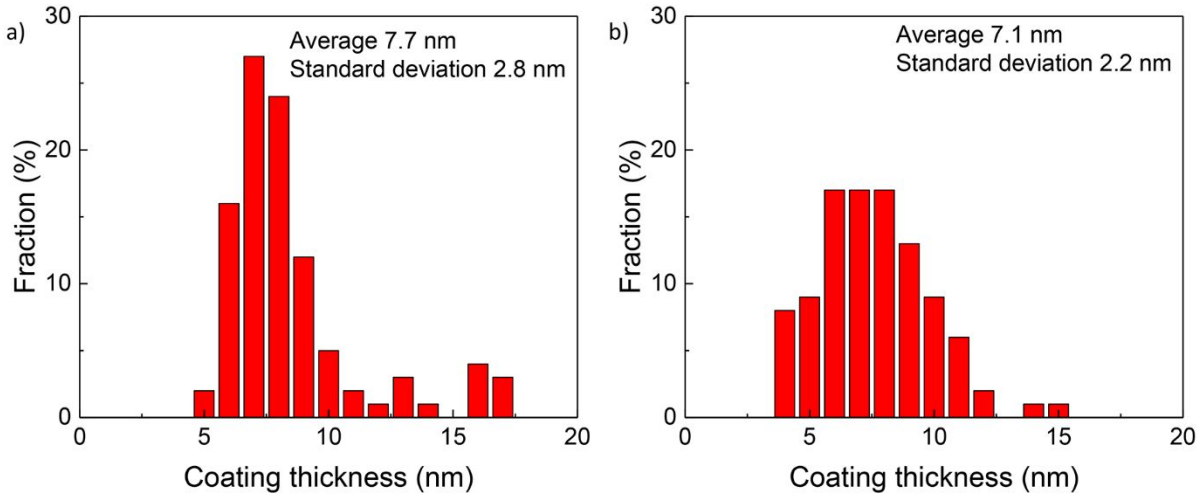

Figure s3. Distribution of the carbon coating thickness as measured by TEM analysis (statistical ensemble of 100 particles) for AC-SNP (a) and GC-SNP (b).

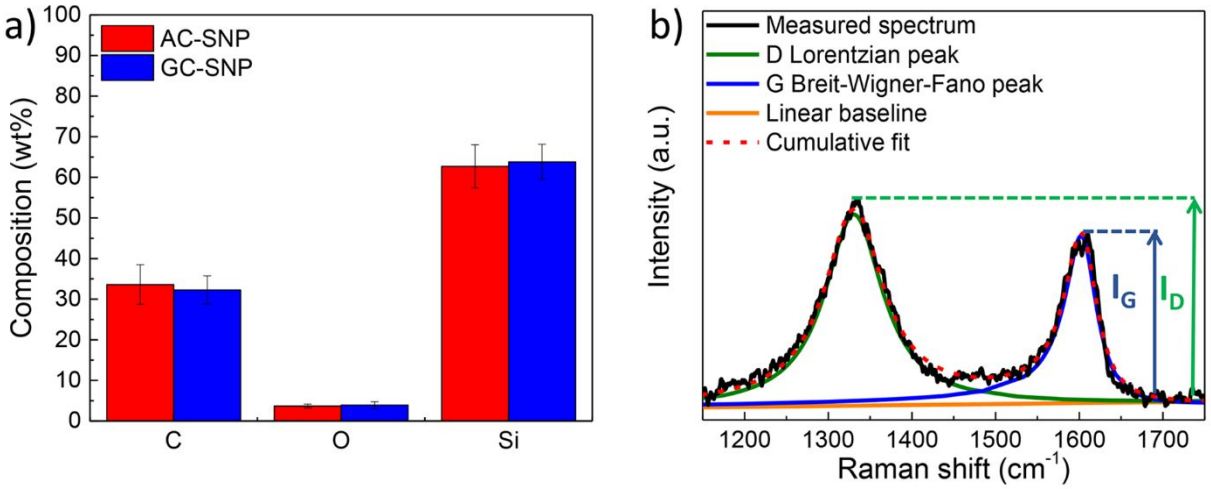

Figure s4. SEM/EDS of the average chemical composition of AC-SNP and GC-SNP (a). Raman fitting procedure employed for the analysis of the graphitization degree of the carbon coating in the synthesized composite materials (b). The fitting procedure encompasses a Lorentzian peak for the D mode, a Breit–Wigner–Fano (BWF) peak for the G mode and a linear baseline.

a)

Analysis method	AC-SNP	GC-SNP	Δ (%)
Raman H (%)	8	5	37.5
FTIR CH_x area (a.u.)	0.26	0.17	34.6

b)

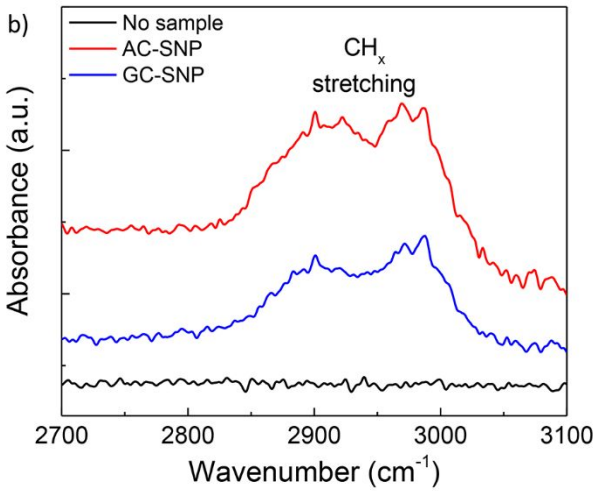

Figure s5. Analysis of the hydrogen content in AC-SNP and GC-SNP via Raman and FTIR analysis (a). Δ is the difference between the hydrogen content of AC-SNP and GC-SNP expressed in percentage. FTIR spectra of AC-SNP and GC-SNP showing the CH_x stretching mode (b).

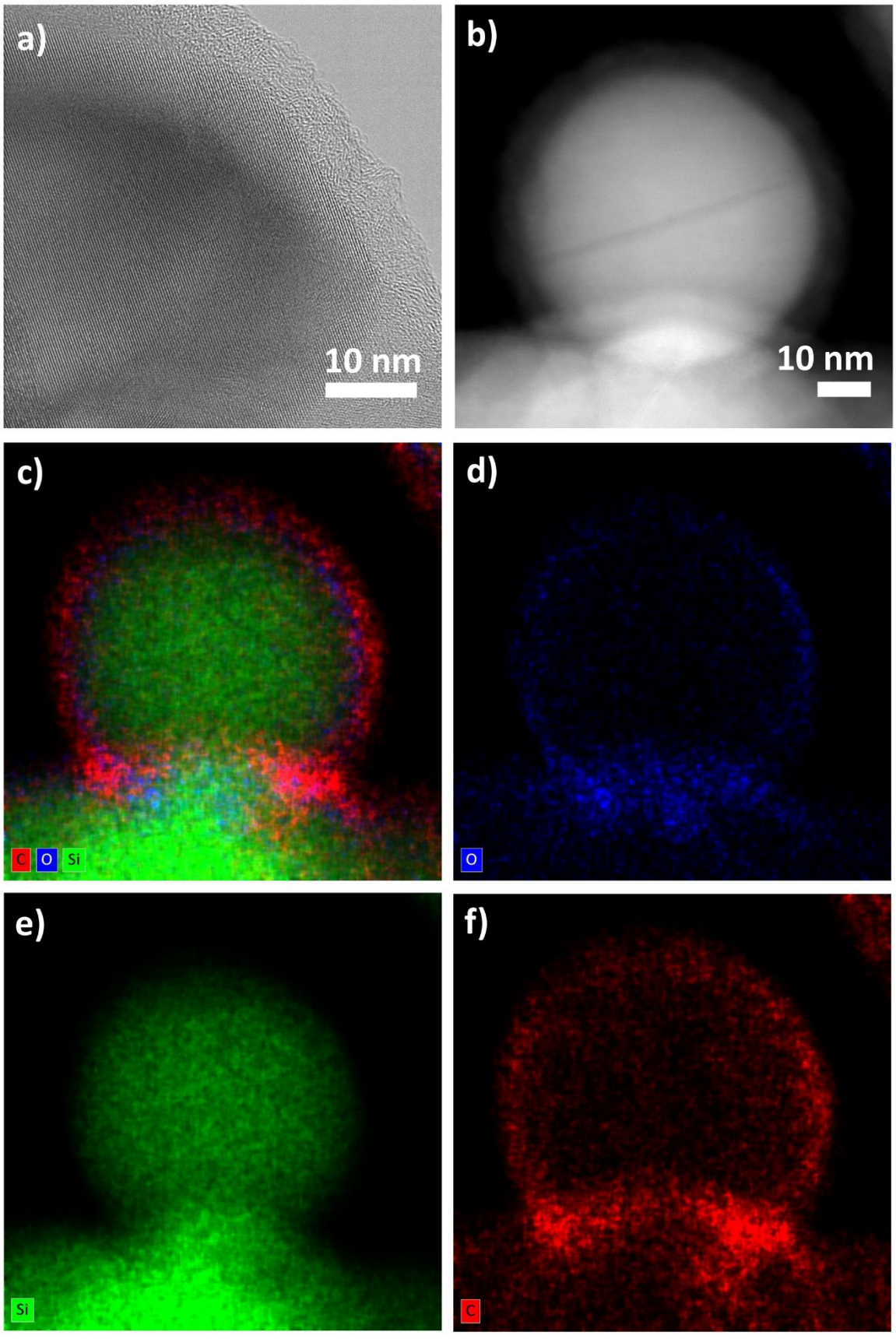
a)
10 nm
b)
10 nm
c)
C O Si
d)
O
e)
Si
f)
C

Figure s6. Bright-field STEM image of a single AC-SNP particle (a). The image highlits the neat interphase between silicon and carbon. Dark field STEM (b) and STEM-EDS micrographs of AC-SNP (c-f).

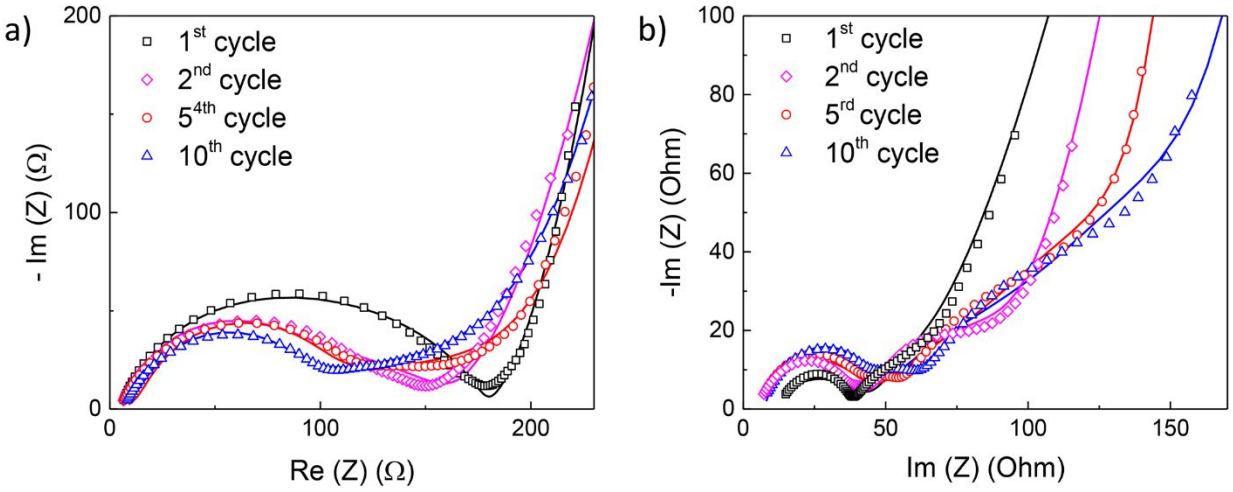

Figure s7. EIS analysis of AC-SNP (a) and GC-SNP (b) after the 1st, 2nd, 5th and 10th lithiation cycles. The fit for each dataset is represented by the corresponding solid line.

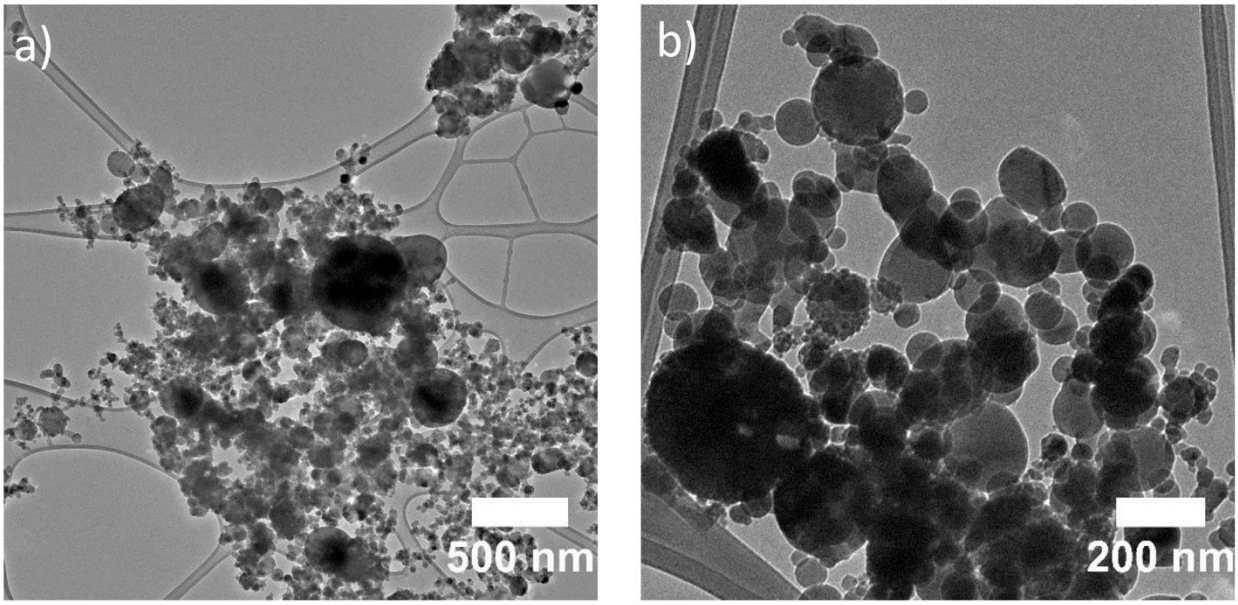

Figure s8. Low magnification TEM micrographs of pristine SNPs.

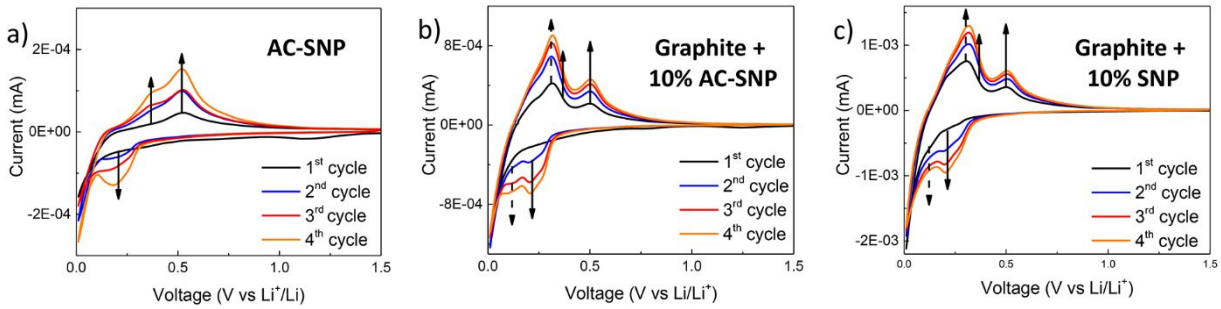

Figure s9. CV curves of electrodes fabricated with AC-SNP (a), graphite +10 wt% AC-SNP (c) and graphite +10 wt% SNP. The solid arrows show the lithiation and delithiation peaks of Si while the broken arrows show the lithiation and delithiation peaks of graphite.